Head and Neck Pathology (2024) 18:48
https://doi.org/10.1007/s12105-024-01634-5

RESEARCH

DNA Mutational and Copy Number Variation Profiling of Primary Craniofacial Osteosarcomas by Next-Generation Sequencing

Gord Guo Zhu[1,2] · Chuanyong Lu[1] · Ivana Petrovic[3] · Khedoudja Nafa[1] · Wen Chen[4] · Aijazuddin Syed[1] · Satshil Rana[1] · Michael J. Klein[5] · Sinchun Huang[6] · Lu Wang[1,7] · William D. Tap[8] · Ronald A. Ghossein[1] · Jatin Shah[3] · Meera R. Hameed[1]

Received: 12 January 2024 / Accepted: 26 February 2024

Abstract

Background Craniofacial osteosarcomas (CFOS) are uncommon malignant neoplasms of the head and neck with different clinical presentation, biological behavior and prognosis from conventional osteosarcomas of long bones. Very limited genetic data have been published on CFOS.

Methods In the current study, we performed comprehensive genomic studies in 15 cases of high-grade CFOS by SNP array and targeted next generation sequencing.

Result Our study shows high-grade CFOS demonstrate highly complex and heterogenous genomic alterations and harbor frequently mutated tumor suppressor genes *TP53, CDKN2A/B, and PTEN,* similar to conventional osteosarcomas. Potentially actionable gene amplifications involving *CCNE1, AKT2, MET, NTRK1, PDGFRA, KDR, KIT, MAP3K14, FGFR1, and AURKA* were seen in 43% of cases. *GNAS* hotspot activating mutations were also identified in a subset of CFOS cases, with one case representing malignant transformation from fibrous dysplasia, suggesting a role for GNAS mutation in the development of CFOS.

Conclusion High-grade CFOS demonstrate highly complex and heterogenous genomic alterations, with amplification involving receptor tyrosine kinase genes, and frequent mutations involving tumor suppressor genes.

Keywords Craniofacial osteosarcoma · Genomics · Next-generation sequencing

✉ Meera R. Hameed
hameedm@mskcc.org

1 Department of Pathology, Memorial Sloan Kettering Cancer Center, New York, NY 10065, USA

2 Department of Pathology, Cooper University Hospital, Cooper Medical School of Rowan University, Camden, NJ 08103, USA

3 Department of Surgery, Memorial Sloan Kettering Cancer Center, New York, NY 10065, USA

4 Department of Pathology, Washington DC VA Medical Center, Washington, DC 20310, USA

5 Department of Pathology, Hospital for Special Surgery, New York, NY 10021, USA

6 Department of Radiology, Memorial Sloan Kettering Cancer Center, New York, NY 10065, USA

7 Department of Pathology, St. Jude Children's Research Hospital, Memphis, TN 38103, USA

8 Department of Medicine, Memorial Sloan Kettering Cancer Center, New York, NY 10065, USA

Introduction

Craniofacial osteosarcomas (CFOS) comprise less than 1% of the malignant neoplasms of head and neck, and approximately 6–7% of all osteosarcomas (OS) [1]. The clinical presentation, biological behavior, and prognosis differ from those conventional OS involving long bones. CFOS preferentially involve maxilla and mandible with swelling, pain, and teeth mobility as the most common clinical presentations. It affects adults at third to fifth decade of life, which is 10–20 years older than conventional long bone OS [1, 2]. CFOS of gnathic bones tend to have more favorable prognosis, longer survival, lower incidence of metastases compared to long bone OS [3]. CFOS are treated with surgical resection, chemotherapy and radiation. Although the role of chemotherapy and radiation in the treatment of CFOS is not well established [4], a recent meta-analysis of thirteen studies with a total of 184 patients showed the five- and ten- year overall survival rates for CFOS are 62% and 49%,

Published online: 17 June 2024

respectively, and chemotherapy could improve survival in patients with a positive margin, high-grade histology or recurrence [5].

CFOS are classified as low grade or high grade by histology and intramedullary or parosteal by location. High-grade OS can be primary or secondary. Secondary CFOS are associated with prior risk factors such as Paget's disease of bone or radiation history, whereas primary CFOS occur de novo without known predisposing factors. Depending on the relative amounts of cartilage, osteoid and collagen produced by tumor cells, high-grade CFOS can be subclassified as chondroblastic, osteoblastic, and fibroblastic subtypes. Other histologic subtypes, such as telangiectatic, small cell, giant cell-rich, and epithelioid have also been described. Histologic type has not been shown to be correlated with patients' prognosis [1].

In recent years, significant progress has been made toward understanding the molecular genetic underpinnings of the OS of long bones through high-throughput sequencing technology. Several studies have shown that the OS of long bones have highly complex and unstable genome with a small number of recurrent gene mutations, including *TP53, RB1, CDKN2A*, and *ATRX* [6–8]. Potentially targetable gene amplifications including *KIT, KDR, PDGFRA*, and *VEGFA* were identified in a subset of OS of long bones [9]. Other recurrent gene alterations occur in less than 5–10% cases, such as *DLG2, MDM2, CDK4, ARID1A, BRCA2, BAP1, RET, MUTYH, ATM, PTEN, WRN, RECQL4, ATRX, FANCA, NUMA1, MDC1, MYC, SOX17,SETD2,* and mutations in insulin-like growth factor (IGF) signaling genes [6–10]. Novel mutation mechanisms, such as chromothripsis (massive genomic rearrangements generated in a single catastrophic event and localized to isolated chromosomal regions) and kataegis (localized hypermutation) have been described in OS of long bones [7].

Very limited genetic data have been reported in CFOS. It is unclear whether CFOS share the same pathophysiology with the conventional OS. No comprehensive genomic analysis has been reported to date in CFOS. In the current study, we performed comprehensive genomic studies on 15 high-grade cases by SNP array and MSK-IMPACT targeted next generation sequencing.

Methods and Materials

Patient Data and Tumor Specimens

The study was conducted after Institutional Review Board approval (#160-1516). The medical records and archived pathological material were retrieved for patients treated during the period between 1990 and 2018 at our institution with a diagnosis of osteosarcoma in the craniofacial bones. The slides and pathological diagnosis from resected specimens were re-reviewed by two pathologists who are subspecialized in bone and soft tissue pathology. They also selected appropriate block for molecular analysis. Fifteen cases with confirmed pathological diagnosis of high-grade OS were included.

SNP Array Analysis

Fifteen cases high-grade CFOS that had sufficient non-decalcified viable tumor tissue available were selected for molecular testing, including 3 radiation associated osteosarcoma cases.

Genomic DNA was extracted from FFPE tumor tissues using Qiagen DNeasy Tissue kit. Genome-wide DNA copy number alterations and allelic imbalances were analyzed by SNP-array using Affymetrix OncoScan Assay (Affymetrix, CA). Eighty nanograms of genomic DNA were used for each sample. Processing of samples was performed according to the manufacturer's guidelines (Affymetrix). OncoScan SNP-array data were analyzed by the software couple of OncoScan Console (Affymetrix) and Nexus Express (BioDiscovery, CA) using Affymetrix TuScan algorithm.

NGS-targeted Sequencing by MSK-IMPACT

Mutation profile analysis of the 14 high-grade CFOS were performed on the MSK-IMPACT platform [11, 12], a validated custom hybridization capture-based assay, which is capable of detecting somatic mutations, small insertions and deletions, copy number alterations, and selected structural rearrangements of 468 genes. Briefly, barcoded sequences are prepared and captured by hybridization with custom biotinylated DNA probes for all exons and selected introns of 468 oncogenes and tumor suppressor genes using 100–250 ng of input DNA. Captured libraries are sequenced on an Illumina HiSeq (2×100 bp paired-end reads). Bioinformatics analysis included alignment of reads to the human genome using BWA-MEM; duplicate read removal, base recalibration, and indel realignment using GATK following best practices; variant calling using MuTect for single nucleotide variants and Somatic Indel Detector for indels. Annovar was used to annotate the variants for cDNA and amino acid changes. Final data were also manually curated to exclude the germline SNP using the following criteria: allele frequency from 0.4 to 0.6 or 0.8 to 1.0 unless the tumor purity is greater than 80% or reported in the gnomAD database more than 10 times. The sequence read alignment processing, non-synonymous mutations, copy number alterations and rearrangements were determined as previously described [11].

Results

Clinicopathologic Features

Of the 15 cases of high-grade CFOS, there were 5 females and 10 males, with ages ranging from 19 to 74 years (median: 52 years). Five tumors were located in maxilla, eight in mandible, and two other locations. The predominant histological subtypes of the high-grade CFOS were osteoblastic (2), chondroblastic (2), and fibroblastic (3). The remaining cases were mixed subtypes. Tumor sizes ranged from 1.5 to 8.0 cm (median 5.3 cm). The detailed clinical and pathological features of 15 cases are summarized in Table 1. Representative radiology images and histology photomicrographs are shown in Fig. 1. All patients underwent surgical resection.

CFOS Demonstrate Highly Complex and Heterogenous Genomic Alterations

All the 15 high-grade CFOS, which were submitted for SNP array analysis, demonstrated highly unstable genome with small- or large-scale copy number alterations (CNAs) and allelic imbalance throughout all the chromosomes (Fig. 2A). The aggregated CNAs and allelic imbalance analyses demonstrated the frequency of recurrent unbalanced genomic aberrations shown in Fig. 2A top panel. While the genomic landscapes appear to be heterogenous from case to case, there were certain patterns seen as large deletions or gains involving whole chromosomes, chromosome arms, or large chromosome segments. Chromosome 1q, 2q, 3q, 5p, 6p, 7, 8, 9q, 19p, 14, 20q, 21 preferentially demonstrated copy number gain (> 50% cases). Chromosome 3p, 5q, 6q, 10, 13, 17p preferentially demonstrated copy number loss (> 50% cases). Chromothripsis, massive genomic rearrangement confined to localized chromosome regions, was observed on multiple chromosomes. Figure 2C demonstrates chromothripsis involving long arm of chromosome 4, which manifests as oscillating copy number alteration between gains and deletions (upper panel) and corresponding interspersed loss of heterozygosity (LOH) at heterozygous SNPs (lower panel).

The CNAs plots from MSK-IMPACT sequencing data of 14 high-grade CFOS also demonstrated similar findings. Figure 2B shows the CNAs plot from one representative CFOS case demonstrating a highly complex and unstable genome with copy number gains or losses involving all the chromosomes. There are also more focal CNAs targeting oncogenes or tumor suppressor genes (discussed in next paragraph).

Table 1 List of all the craniofacial osteosarcoma cases included in the current study

Number	Sex	Age (years)	Site	Histology	Grade	Tumor size (cm)	Molecular studies
1	M	19	Mandible	Osteoblastic	High	11	MSK-IMPACT, SNP Array
2	M	58	Maxilla	Osteoblastic, Chondroblastic (RT associated)	High	4.2	MSK-IMPACT, SNP Array
3	M	67	Mandible	Osteoblastic, Chondroblastic, Fibroblastic (RT associated)	High	6.5	MSK-IMPACT, SNP Array
4	F	54	Maxilla	Osteoblastic	High	1.5	MSK-IMPACT, SNP Array
5	M	54	Mandible	Chondroblastic, Osteoblastic, Fibroblastic (RT associated)	High	3.5	MSK-IMPACT, SNP Array
6	F	22	Mandible	Osteoblastic, Chondroblastic	High	6.5	MSK-IMPACT, SNP Array
7	M	52	Frontal sinus and infratemporal fossa	Osteoblastic, Chondroblastic, Fibroblastic	High	7	MSK-IMPACT, SNP Array
8	F	37	Mandible	Fibroblastic, Osteoblastic, Chondroblastic	High	5.3	MSK-IMPACT, SNP Array
9	F	74	Maxilla	Fibroblastic	High	6.5	MSK-IMPACT, SNP Array
10	M	52	Maxilla	Osteoblastic, Chondroblastic, Fibroblastic	High	4	MSK-IMPACT, SNP Array
11	M	24	Mandible	Fibroblastic	High	8	MSK-IMPACT, SNP Array
12	M	43	Maxilla	Chondroblastic	High	4.5	MSK-IMPACT, SNP Array
13	M	25	Mandible	Chondroblastic	High	5.5	SNP Array
14	M	67	Mandible	Fibroblastic	High	5.3	MSK-IMPACT, SNP Array
15	F	29	Sphenoid wing	Osteoblastic, Chondroblastic	High	2.9	MSK-IMPACT

Cases #10 and #15 are the cases in which *GNAS* hotspot mutations were identified. The Case #10 had history of fibrous dysplasia since age of 11, in which histology of fibrous dysplasia is present on the H&E slide

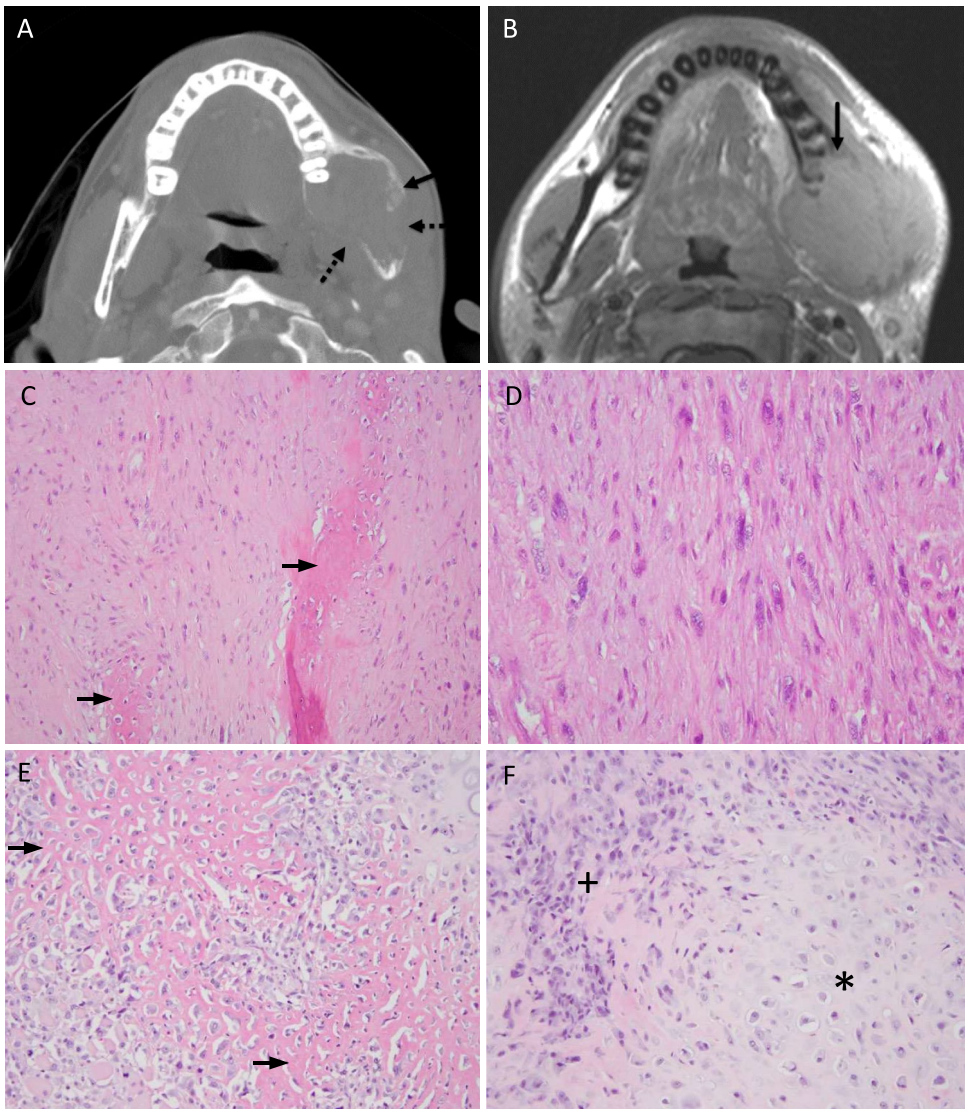

Fig. 1 Representative radiology and H&E histology images of CFOS of maxilla. **A** An axial contrast-enhanced CT image shows a 5.0 × 3.2 cm expansile lytic lesion causing cortical destruction (dotted arrows) and cortical thinning in the left mandible. The lesion contains a focus of sclerosis (arrow) and abuts the left molar root. **B** An axial non-contrast T1-weighted image demonstrates the lesion with a cortical destruction (arrow) and indistinguishable from the adjacent muscles; **C**, **D** H&E images (200x, 400x) of a high grade fibroblastic osteosarcoma composed of predominantly of spindle cells with focal pleomorphism and focal neoplastic osteoid (arrows); **E** H&E image (400x) of a high grade osteoblastic CFOS composed of highly pleomorphic epithelioid tumor cells surrounded individually by eosinophilic lace-like neoplastic osteoid (arrows); **F** H&E image (400x) of a high grade chondroblastic CFOS composed of chondroid area (asterisk) and peripheral early osteoid formation (plus sign). The chondroid area consists of pleomorphic epithelioid tumor cells in the light blue chondroid matrix, while immature osteoid matrix is seen around the angular/spindly atypical tumor cells at the periphery of the chondroid area

Somatic Gene Mutations and Potentially Targetable Oncogene Amplifications

The number of non-synonymous mutations (SNV or small indels) ranged from 1 to 10 per case (median: 3 / case, median tumor mutation burden: 2.6 / Mb). The most frequently mutated gene was *TP53* (79%, 11/14), alterations of which include missense mutations ($n = 8$), frameshift truncation ($n = 1$), in-frame deletion ($n = 1$), and splice variant ($n = 1$) (Fig. 3). These mutations were often accompanied by LOH at chromosome level (17p loss, affecting *TP53* at 17p13, as shown in chromosome CNAs section). Other recurrently altered genes occurred at lower frequencies (2–3 cases /14), including *CDKN2A/2B* homozygous deletion, *TERT* amplification or hotspot mutation in the promoter, *PBRM1* frameshift truncations, *KMT2C* missense mutations, *APC* missense mutations, *GNAS* hotspot mutations, *PTEN* homozygous deletion, frameshift truncation and missense mutation, *RB1* homozygous deletion, missense mutation and in-frame deletion, and *RAD50* missense mutation and in-frame fusion. These recurrently mutated genes can be categorized into RAS-PI3K, cell cycle, DNA repair, and epigenetic regulation pathways, respectively, based on their biological functions.

Six out of fourteen (43%) cases had at least one potentially actionable oncogene amplification, including *CCNE1, AKT2, MET, NTRK1, PDGFRA, KDR, KIT, MAP3K14, FGFR1, and AURKA*, most of which encode protein kinases (Fig. 4). *PDGFRA, KDR,* and *KIT* were co-amplified in one amplicon on chromosome 4p16 in one case. No clear association was found between genetic alterations and histologic types for most cases, except two cases (see next paragraph).

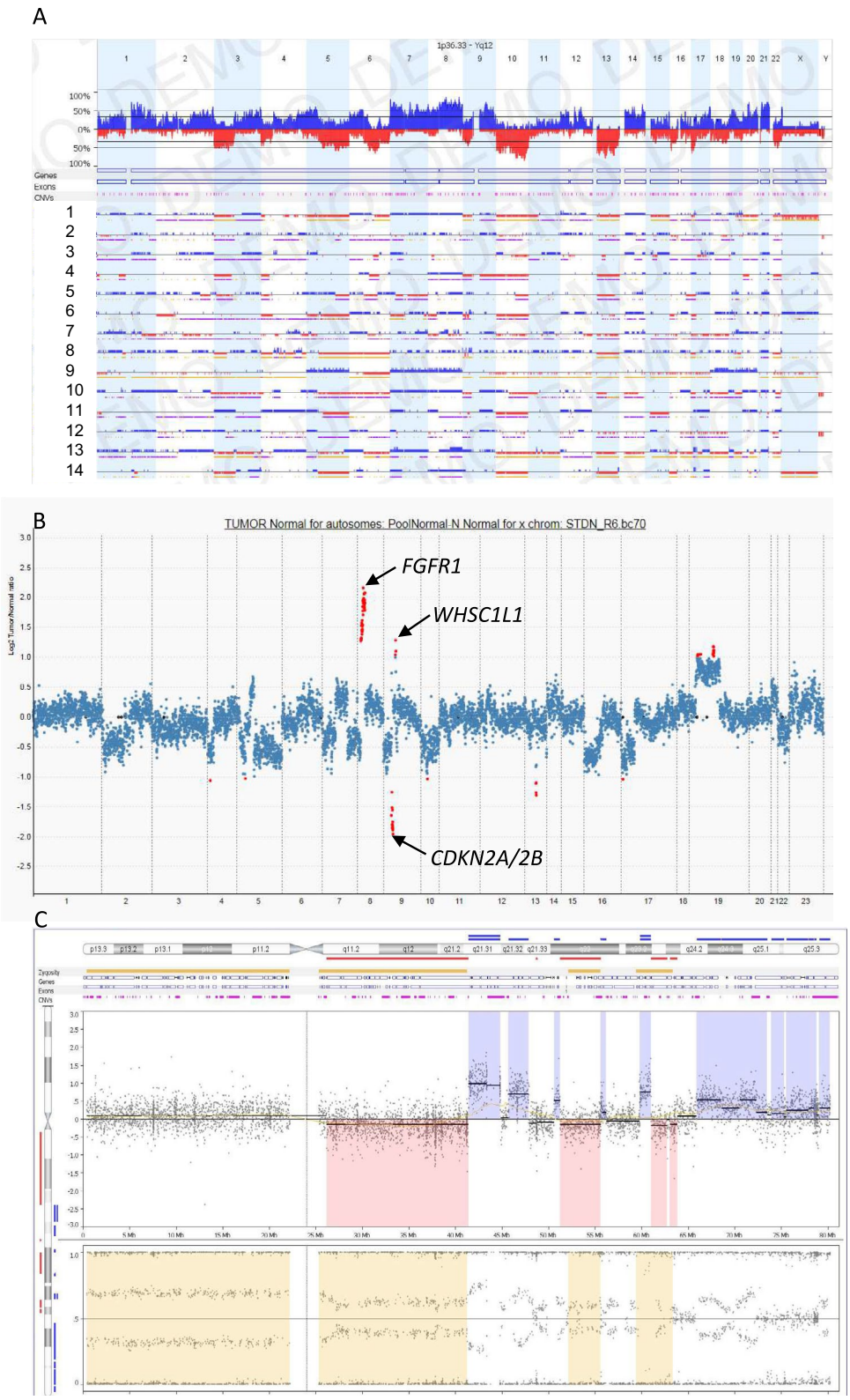

Fig. 2 CNAs by SNP array and representative copy number alteration by MSK-IMPACT in one CFOS case. **A** Genome-wide frequency plot of DNA copy number gains (blue) and losses (red) for 14 CFOS cases by SNP array with chromosomes organized in columns and indicated by labels on the top. **B** Copy number plot of a representative CFOS case using MSK-IMPACT NGS sequencing data (y axis: log2 (tumor/normal ratio), x axis: chromosome#). This particular case of CFOS shows complex chromosomal alterations, and relatively focal *FGFR1* and *WHSC1L1* amplification and deletion of *CDKN2A/2B*. **C** Chromothripsis involving long arm of chromosome 4, shows oscillating CNAs between gains and deletions (upper panel) and corresponding interspersed LOH at heterozygous SNPs (lower panel)

GNAS Activating Mutations in CFOS

GNAS hotspot activating mutations (R201C, R201H), which are the most common driver mutations in fibrous dysplasia, were found in two high-grade CFOS (Fig. 5A, B). Interestingly, both cases had concurrent mutations in *TP53* and *APC,* suggesting possible synergistic effect among these three genes during the development of CFOS. *RB1*, *TGFB1*,

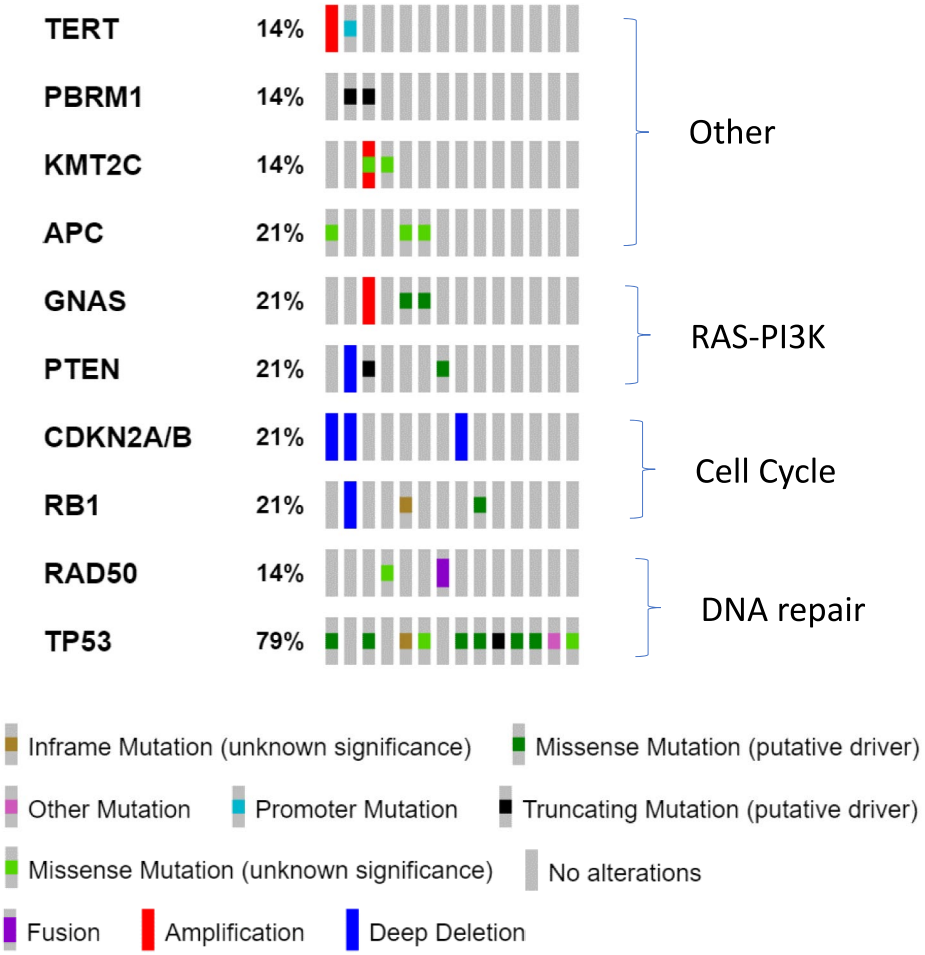

Fig. 3 Oncoprint plot of recurrently mutated genes in 14 high-grade CFOS grouped in signaling pathways

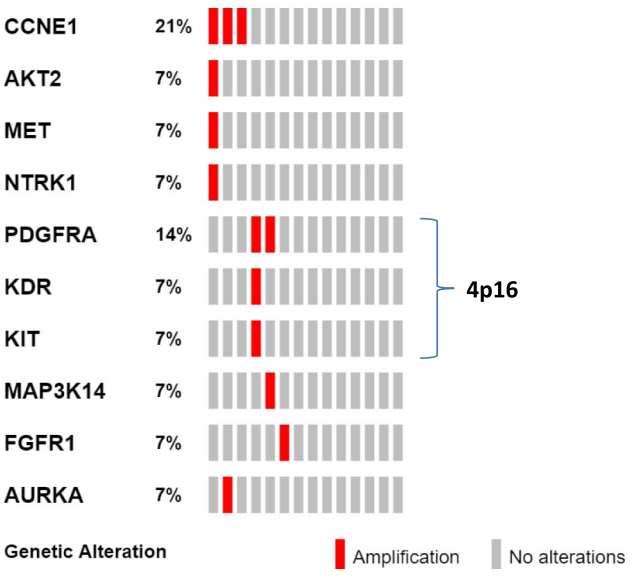

Fig. 4 Oncoprint plot of potentially targetable gene amplifications in 14 high-grade CFOS

and *CBL* were other mutated genes that occurred only in one case. We were able to identify fibrous dysplasia component in one case upon histology review. This was a 7 cm large destructive tumor of left maxilla from a 52-year-old male, who had history of fibrous dysplasia since age of 11. The morphology was that of a high-grade osteosarcoma with features of undifferentiated pleomorphic sarcoma in a background of fibrous dysplasia (Fig. 5C). The second case was a 29-year-old female with a skull base tumor (infratemporal fossa) which showed high-grade osteosarcoma with osteoblastic and chondroblastic differentiation.

Localized Hypermutation in *APC*

One of the mutant *APC* alleles, identified in one case of the high-grade CFOS, demonstrated 8 missense mutations within a range of approximately 2500 base pairs (Fig. 6). Six of eight nucleotide substitutions were "G > A" (or "C > T" on the complementary strand) transitions and two were "G > C" (or "C > G" on the complementary strand) transversions. Two of the mutations were 10 base pairs apart (genomic

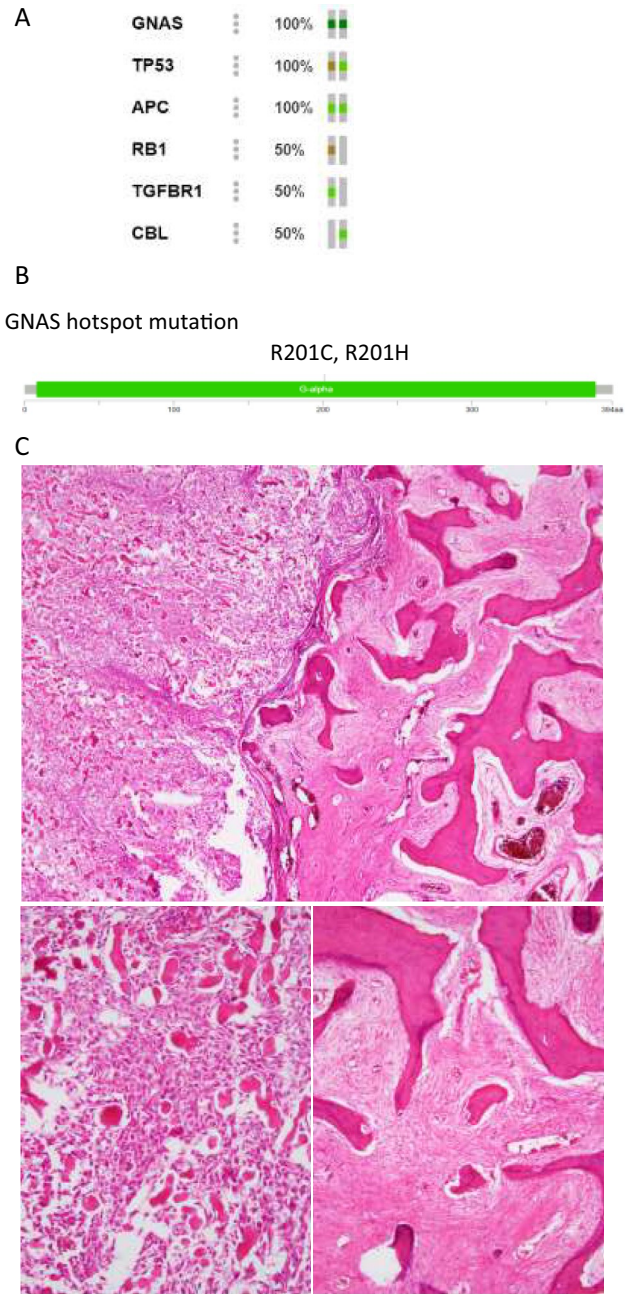

Fig. 5 **A** Two cases of CFOS with *GNAS* hotspot mutations and concurrent mutations; **B** Schematic of GNAS protein and its hotspot mutations; **C** Representative H&E images of one CFOS case with area of fibrous dysplasia, top panel: 40x, bottom left: 200×of osteosarcoma area, bottom right: 100×of fibrous dysplasia area

coordinates: cgr5:112,173,830 and chr5:112,173,840), and were located on the same allele (in *cis*, Fig. 6C). The distances between other mutations were greater than the length of reads of our sequencing platform (150 base pairs on average) so that whether they were *in trans* or *in cis* could not be determined. This localized cluster of hypermutations, with exclusive "C > T" and "C > G" substitution, and likely being in *cis*, is highly suggestive a kataegis event targeting the tumor suppressor gene *APC*.

Discussion

Most conventional OS of long bones are high-grade sarcomas that produce neoplastic osteoid and demonstrate nuclear pleomorphism, frequent mitotic figures including atypical mitoses, and intratumoral and intertumoral heterogeneity by morphology. These histomorphologic abnormalities are phenotypic expression of their underlying aneuploidy and genomic instability. These hallmarks of OS have been well studied through traditional technologies, such as karyotyping, comparative genomic hybridization, fluorescence in situ hybridization, and quantitative PCR. In recent years, high-throughput NGS-based molecular diagnostic tests have been utilized to systematically analyze the gene mutations, CNAs, and structural variants in conventional OS of long bones [6–10]. These studies have confirmed our previous understanding of genomic instability in OS. As far as our knowledge or search in literature, the current study is the first comprehensive genomics analyses on CFOS, using both SNP array or targeted NGS sequencing technology, which demonstrate that, high-grade CFOS also harbor highly unstable and complex genomes, like their long bone counterparts. In CFOS we identified some of the chromosomal alterations have been recurrently identified in OS of long bones, such as gain of 6p, gain of 8p, loss of 17p [13]. Relevant oncogenes or tumor suppressor genes are located in these recurrent chromosomal regions, for instance, *RUNX2, VEGFA, E2F3*, and *CDC5L* on 6p, *MYC* on 8q, and *TP53* on 17p.

We also observed chromothripsis and kataegis (the localized hypermutation seen in APC gene) in the present study, which suggests similar molecular mechanisms might account for the aneuploidy/genomic instability of CFOS. Chromothripsis is characterized by massive genomic rearrangement confined to a localized chromosome region after a one-off catastrophic chromosomal breakage [14–16]. Chromothripsis results in multiple oscillations between two or three copy number states on the affected chromosome. It is estimated that chromothripsis can be seen in at least 2%–3% of all cancers and is present in approximately 25% of bone cancers [15]. Chromothripsis is found to be the molecular mechanism initiating the chromosomal complexity of conventional OS of long bones in > 90% of cases [8, 10]. Chromothripsis has been shown to generate genomic consequences that promote cancer development. The preferential gain or loss of certain chromosome or arms seen in the CFOS may be a selection result of growth advantage conferred by gain of oncogenes or loss of tumor suppressor genes, such as *MYC* on 8q and *TP53* on chromosome 17p.

A

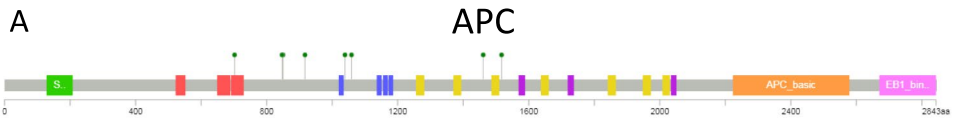

B

Gene	Protein Change	Start Pos	End Pos	Ref	Var	Mutation Type	Allele Freq
APC	E1461K	112175672	112175672	G	A	Missense_Mutation	0.05
APC	D917N	112174040	112174040	G	A	Missense_Mutation	0.08
APC	G702E	112173396	112173396	G	A	Missense_Mutation	0.05
APC	E847K	112173830	112173830	G	A	Missense_Mutation	0.06
APC	R850T	112173840	112173840	G	C	Missense_Mutation	0.06
APC	G1039R	112174406	112174406	G	A	Missense_Mutation	0.05
APC	E1059K	112174466	112174466	G	A	Missense_Mutation	0.07
APC	Q1517H	112175842	112175842	G	C	Missense_Mutation	0.05

C

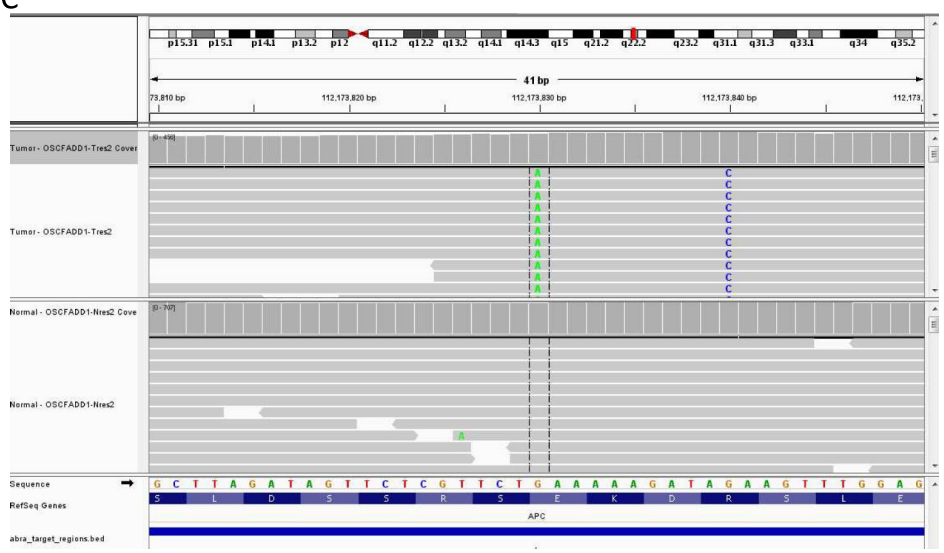

Fig. 6 Localized hypermutations in *APC* in one CFOS case, top panel: lollipop plot demonstrates locations of the mutant amino acid residues on the protein; middle panel: detailed information on the mutations; lower panel: IGV view of the NGS reads showing two adjacent mutations are in *cis*

CFOS in this study have a median of 3 non-synonymous mutation counts / case (median tumor mutation burden: 2.6 / Mb), which places it at low to intermediate level in terms of tumor mutation burdens when compared to other human cancers [17]. The only mutated gene with high recurrent frequency is *TP53*, the guardian of genome stability [18], which is frequently found to be mutated in various human cancers including ones showing chromothripsis [19]. Other mutations occur at much lower frequencies, including amplification of oncogenes which are potentially targetable. The relative low tumor mutation burden of CFOS is also consistent with findings from OS of long bones [20], which place OS in the "cold tumor' category with possibly limited potential for immune checkpoint inhibitors such as PD-L1 inhibitors. A recent clinical trial (NCT02301039) shows that only 1 in 22 advanced OS treated with pembrolizumab (PD1 inhibitor) had partial response [21].

We identified *GNAS* hotspot activating mutations in two CFOS cases and identified fibrous dysplasia component on histology in one patient who had prior history of fibrous dysplasia. Malignant transformation of FD to OS or other sarcomas has been well documented in the literature with frequency varying from less than 1% to 6.7% [22–24]. *GNAS* hotspot mutations were identified in both the fibrous dysplasia and sarcoma components in majority of reported cases (8/10) [25]. Consistent with our findings, *TP53* inactivating mutations, multiple CNAs, and multiple chromosomal abnormalities have been reported in the prior studies [25, 26]. Although structural variants involving *GNAS* have been shown, de novo *GNAS* activating mutations have not been reported in the previous comprehensive genomics studies of long bone OS [6–9]. Majority of fibrous dysplasia cases harbor *GNAS* R201C/R201H activating mutations [27, 28], which are known driver mutations in the development of fibrous dysplasia. *GNAS* encodes the alpha-subunit of the heterotrimeric G protein complex. The missense mutation at residue R201 causes constitutive activation of the G-stimulatory pathway with increased cAMP production

[29], which will disrupt the normal self-renewal process of skeletal stem cells [30]. It is possible that *GNAS* activating mutations, might cooperate with *APC* and *TP53* inactivation in malignant transformation to high-grade CFOS based on the observation from the current study. Studies using genetically engineered mouse models with combination of *GNAS* hotspot mutations with or without knockout of *APC* and *TP53* can further elucidate the role of *GNAS*, as well as any synergistic role of *APC* and *TP53* inactivation, in the malignant transformation of fibrous dysplasia to CFOS.

In summary, high-grade CFOS demonstrate highly unstable and complex genomes, recurrently mutated genes including *TP53, CDKN2A/B, and PTEN,* and gene amplifications in *CCNE1, AKT2, MET, NTRK1, PDGFRA, KDR, KIT, MAP3K14, FGFR1, and AURKA,* leading to activation of the RAS-PI3K pathway, or aberrations in the cell cycle, DNA repair, and epigenetic regulation pathways. Thus potentially targetable genetic events (*PDGFRA, KIT, FGFR1, PTEN*) are present similar to high-grade OS of long bones. Further studies with a larger cohort are needed for the true prevalence of these targetable genetic alterations.

Acknowledgements This research was funded in part through the National Institutes of Health/National Cancer Institute Cancer Center Support Grant P30 CA008748.

Author contributions All authors contributed to the study conception and design. Material preparation, data collection and analysis were performed by G.G.Z. and M.H.. The draft and figures of the manuscript was written and prepared by G.G.Z., and finalized by G.G.Z. and M.H.. All authors read, made comments and approved the final manuscript.

Data availability Data is provided within the manuscript or supplementary information files.

Declarations

Conflict of interest The authors have no relevant conflicts of interest to disclose.

Ethical Approval and Consent to Participate The study was conducted after Institutional Review Board approval (#160–1516). The study was performed in accordance with the Declaration of Helsinki.

References

1. Neville BW et al (2016) Oral and maxillofacial pathology, vol xiii, 4th edn. Elsevier, St. Louis, p 912
2. Czerniak B, Dorfman HD (2016) Dorfman and Czerniak's bone tumors, vol xiii, 2nd edn. Elsevier, Philadelphia, p 1506
3. Hameed M, Horvai AE, Jordan RCK (2020) Soft tissue special issue. Head Neck Pathol 14:70–82
4. Lee RJ et al (2015) Characteristics and prognostic factors of osteosarcoma of the jaws: a retrospective cohort study. JAMA Otolaryngol Head Neck Surg 141(5):470–477
5. Liang L et al (2019) An individual patient data meta-analysis on the effect of chemotherapy on survival in patients with craniofacial osteosarcoma. Head Neck 41(6):2016–2023
6. Bousquet M et al (2016) Whole-exome sequencing in osteosarcoma reveals important heterogeneity of genetic alterations. Ann Oncol 27(4):738–744
7. Chen X et al (2014) Recurrent somatic structural variations contribute to tumorigenesis in pediatric osteosarcoma. Cell Rep 7(1):104–112
8. Kovac M et al (2015) Exome sequencing of osteosarcoma reveals mutation signatures reminiscent of BRCA deficiency. Nat Commun 6:8940
9. Suehara Y et al (2019) Clinical genomic sequencing of pediatric and adult osteosarcoma reveals distinct molecular subsets with potentially targetable alterations. Clin Cancer Res 25(21):6346–6356
10. Behjati S et al (2017) Recurrent mutation of IGF signalling genes and distinct patterns of genomic rearrangement in osteosarcoma. Nat Commun 8:15936
11. Cheng DT et al (2015) Memorial sloan kettering-integrated mutation profiling of actionable cancer targets (MSK-IMPACT): a hybridization capture-based next-generation sequencing clinical assay for solid tumor molecular oncology. J Mol Diagn 17(3):251–264
12. Zehir A et al (2017) Mutational landscape of metastatic cancer revealed from prospective clinical sequencing of 10,000 patients. Nat Med 23(6):703–713
13. Board WCOTE (2020) *Soft Tissue and Bone Tumours: WHO Classification of Tumours*. International Agency for Research on Cancer
14. Korbel JO, Campbell PJ (2013) Criteria for inference of chromothripsis in cancer genomes. Cell 152(6):1226–1236
15. Stephens PJ et al (2011) Massive genomic rearrangement acquired in a single catastrophic event during cancer development. Cell 144(1):27–40
16. Zhang CZ et al (2015) Chromothripsis from DNA damage in micronuclei. Nature 522(7555):179–184
17. Schumacher TN, Schreiber RD (2015) Neoantigens in cancer immunotherapy. Science 348(6230):69–74
18. Strachan T, Read AP (2019) Human molecular genetics, vol xiii, 5th edn. CRC Press, Taylor & Francis Group, Boca Raton, p 770
19. Cortes-Ciriano I et al (2020) Comprehensive analysis of chromothripsis in 2,658 human cancers using whole-genome sequencing. Nat Genet 52(3):331–341
20. Perry JA et al (2014) Complementary genomic approaches highlight the PI3K/mTOR pathway as a common vulnerability in osteosarcoma. Proc Natl Acad Sci U S A 111(51):E5564–E5573
21. Tawbi HA et al (2017) Pembrolizumab in advanced soft-tissue sarcoma and bone sarcoma (SARC028): a multicentre, two-cohort, single-arm, open-label, phase 2 trial. Lancet Oncol 18(11):1493–1501
22. Ruggieri P et al (1994) Malignancies in fibrous dysplasia. Cancer 73(5):1411–1424
23. Qu N et al (2015) Malignant transformation in monostotic fibrous dysplasia: clinical features, imaging features, outcomes in 10 patients, and review. Medicine (Baltimore) 94(3):e369
24. Tanner HC Jr, Dahlin DC, Childs DS Jr (1961) Sarcoma complicating fibrous dysplasia. Probable role of radiation therapy. Oral Surg Oral Med Oral Pathol 14:837–46
25. Shi R et al (2022) Clinicopathological and genetic study of a rare occurrence: malignant transformation of fibrous dysplasia of the jaws. Mol Genet Genomic Med 10(1):e1861
26. Yap FHX et al (2021) Malignant transformation of fibrous dysplasia into osteosarcoma confirmed with TP53 somatic mutation and mutational analysis of GNAS gene. Pathology 53(5):652–654
27. Lee SE et al (2012) The diagnostic utility of the GNAS mutation in patients with fibrous dysplasia: meta-analysis of 168 sporadic cases. Hum Pathol 43(8):1234–1242

28. Jour G et al (2016) GNAS mutations in fibrous dysplasia: a comparative study of standard sequencing and locked nucleic acid PCR sequencing on decalcified and nondecalcified formalin-fixed paraffin-embedded tissues. Appl Immunohistochem Mol Morphol 24(9):660–667
29. Lyons J et al (1990) Two G protein oncogenes in human endocrine tumors. Science 249(4969):655–659
30. Kuznetsov SA et al (2008) Age-dependent demise of GNAS-mutated skeletal stem cells and "normalization" of fibrous dysplasia of bone. J Bone Miner Res 23(11):1731–1740